Vibration Suppression Design for Virtual Compliance Control in Bilateral Teleoperation

Chanuphon Trakarnchaiyo

Mechatronics, Industrial Systems Engineering
Asian Institute of Technology
Pathumthani, Thailand
e-mail: st117779@ait.asia

A. M. Harsha S. Abeykoon

Mechatronics, Industrial Systems Engineering
Asian Institute of Technology
Pathumthani, Thailand
e-mail: harsha@ait.asia

Abstract—**Disturbance rejection is an important technique in bilateral teleoperation that can ensure the stability of the system from unwanted inputs. One of the major disturbance for the system is the external vibration from both sides. This paper aims to apply the concept of one degree-of-freedom inertia-spring-damper system for vibration suppression in the bilateral control system. For vibration control, the system compliance for different input frequency is controlled by the value of virtual elements which is designed based on the cut-off frequencies and stiffness of the virtual spring. The performance of the proposed bilateral control system with different virtual parameters is verified through simulation.**

Keywords—vibration suppression; virtual model; compliance control; bilateral teleoperation

I. INTRODUCTION

Since the teleoperation has been studied by several researchers throughout many decades, this system allows the human to manipulate the machine from a distance that benefits for humankind in various fields. Exploration robots in space and underwater, unmanned ground/air vehicles for landmine destruction and surveillance are some of the applications where the teleoperation is used. Furthermore, with the advancement in medical and robotics technology, the surgical operation called minimally invasive surgery can be performed by a robot system controlled by the surgeon from a distance, which is commonly known as telesurgery [1]. Especially, the ability to reflect the sense of touch from the environment to the operator is the most important feature for teleoperation. This feature can be attained by using the two-way control system or more specifically using *bilateral control*.

Generally, the bilateral control system consists of five parts: human, master system, communication channel, slave system, and environment. The data from both master and slave sides is exchanged via the communication channel to control the other side as shown in Fig. 1. According to a survey [2], several bilateral control concepts were proposed, however, two indices, namely stability and transparency, are mainly used to evaluate the controller performance. For the early bilateral control was designed in two-port network model [3], [4]. The stability of the control system is the important part of that research. Next, the control system was extended the communication ports to be the four-channel

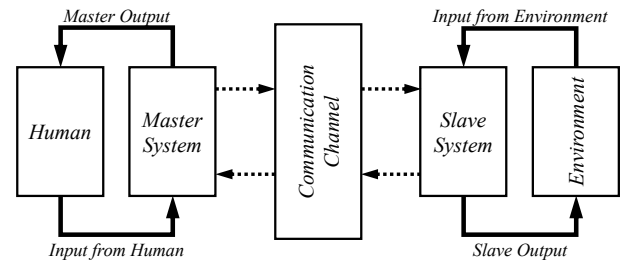architecture in [5], which is used to improve the transparency of the system.

Figure 1. Bilateral control system overview.

However, the stability of the bilateral control can be ruined from unwanted disturbances, namely internal disturbances and external disturbances. For internal disturbances, the uncertainty of system parameters and unknown parameters that do not be included when designing the control system can affect the stability of the system. Similarly, the system can become unstable when external disturbances such as unexpected inputs or contaminated input with vibration noise act on the system from both master and slave sides. Hence, several studies on disturbance rejection for bilateral teleoperation were proposed. For instance, the Disturbance Observer (DOB) [6] uses the difference between current command and actual position output to calculate for the disturbance torque and compensate. This DOB technique was improved to handle noises in [7]. Next, the concept of a low-pass filter can be applied for vibration suppression in [8]. Moreover, several adaptive controllers for internal and external disturbance rejections are detailed in [9].

In mechanical systems, a shock absorber which normally consists of spring and damper is used for vehicle suspension. The concept of spring-damper system was applied to design the bilateral control system for soft manipulation [10]. Nevertheless, the details of vibration suppression analysis were not discussed. Therefore, in this paper, the one degree-of-freedom spring-damper system with additional inertia for both master and slave side is adopted to design the bilateral control system. For the design method, the disturbance suppression performance of the proposed bilateral control depends on the value of virtual parameters which are determined from the desired cut-off frequencies and virtual spring stiffness. Frequency response of the modified bilateral

control system is analyzed in this paper. Further, the effects of the virtual parameters are also analyzed.
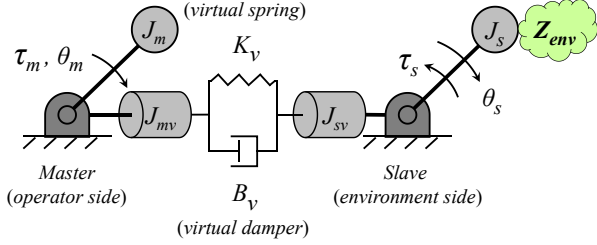

Figure 2.   Inertia-Spring-Damper system model with virtual parameters.

The remaining of this paper is organized as follows; in section II, the inertia-spring-damper system is introduced to design the bilateral control system and the analysis of this proposed control is described in section III. Section IV explains the vibration suppression design of the proposed bilateral control. In section V, the performance of this control is verified through the simulations. Finally, this paper is concluded in section VI.

II.   SYSTEM MODELING

A. Inertia-Spring-Damper System Model

For the inertia-spring-damper system as shown in Fig. 2, the master and slave systems have the system inertia, J_m and J_s, respectively. The additional inertia, J_{mv} and J_{sv}, is attached to both sides of the system. Moreover, these two systems are interconnected with the damper, B_v and spring, K_v. Therefore, the dynamics equation of master side is (1).

$$(J_m + J_{mv})s^2\theta_m = \tau_m + (B_v s + K_v)(\theta_s - \theta_m) \qquad (1)$$

For slave side, the dynamics equation is expressed as (2).

$$(J_s + J_{sv})s^2\theta_s = -\tau_s + (B_v s + K_v)(\theta_m - \theta_s) \qquad (2)$$

where τ and θ denote the torque and position, s is Laplace operator, and subscript m, s and v represents the parameters of master, slave and virtual, respectively.

B. Bilateral Control Scheme

From (1) and (2), additional inertia, damper, and spring are considered as virtual elements in the controller. the system equation can be rearranged for the proposed bilateral control system as expressed in (3) and (4).

$$J_m s^2\theta_m = \tau_m + [(B_v s + K_v)(\theta_s - \theta_m) - J_{mv}s^2\theta_m] \qquad (3)$$

$$J_s s^2\theta_s = -\tau_s + [(B_v s + K_v)(\theta_m - \theta_s) - J_{sv}s^2\theta_s] \qquad (4)$$

where the external torques are action and reaction torque of human and environment impedance, Z_h and Z_{env}, respectively. Moreover, the external torque can be contaminated by a disturbance torque and it could disturb the stability of the system. The latter part of system equation is the torque from the virtual elements.

Therefore, from (3) and (4), the block diagram of the proposed bilateral control system can be constructed as

depicted in Fig. 3. Delay time in communication channel is not considered in this paper.
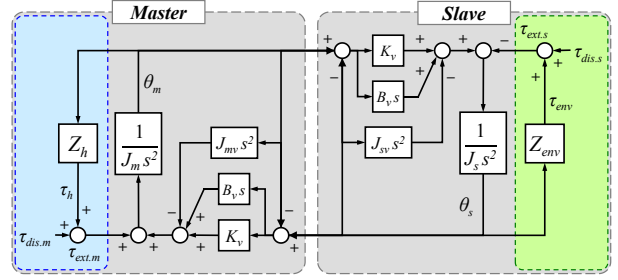

Figure 3.   Block diagram of proposed bilateral control system.

The proposed bilateral controller utilizes the concept of position error based torque reflection to the operator at the master side which is similar to [11]. However, the resultant reflection and effort torque to human and environment side are different from the additional torque of virtual inertia.

III.   PROPOSED BILATERAL CONTROLLER ANALYSIS

Typically, the bilateral control system can be represented by 2×2 matrix [3], [4]. From (3) and (4), the hybrid matrix with hybrid parameters, H, of the proposed bilateral control system is expressed as (5).

$$\begin{bmatrix} \tau_m \\ \theta_s \end{bmatrix} = \begin{bmatrix} H_{11} & H_{12} \\ H_{21} & H_{22} \end{bmatrix} \begin{bmatrix} \theta_m \\ -\tau_s \end{bmatrix} \qquad (5)$$

where

$$H_{11} = \frac{1}{Z_s}[Z_m Z_s - (B_v s + K_v)^2] \qquad (6)$$

$$H_{12} = -\frac{1}{Z_s}[B_v s + K_v] \qquad (7)$$

$$H_{21} = \frac{1}{Z_s}[B_v s + K_v] \qquad (8)$$

$$H_{22} = \frac{1}{Z_s} \qquad (9)$$

and

$$Z_m = (J_m + J_{mv})s^2 + B_v s + K_v \qquad (10)$$

$$Z_s = (J_s + J_{sv})s^2 + B_v s + K_v \qquad (11)$$

Recall the condition of transparency is defined from the transmitted impedance, Z_t which is transferred to the operator should be equal to the environment impedance, Z_{env} [5].

$$Z_t = Z_{env} = \frac{\tau_s}{\theta_s} \qquad (12)$$

The relationship of the transmitted impedance and the environment impedance can be found by rewriting the equation from the hybrid matrix (5) as expressed in (13).

$$Z_t = \left(\frac{-H_{12}H_{21}}{1 + H_{22}Z_{env}} \right) Z_{env} + H_{11} \qquad (13)$$

Hence, the value of hybrid parameters should be derived as shown in (14) to achieve the perfect transparency condition.

$$\begin{bmatrix} \tau_m \\ \theta_s \end{bmatrix} = \begin{bmatrix} 0 & -1 \\ 1 & 0 \end{bmatrix} \begin{bmatrix} \theta_m \\ -\tau_s \end{bmatrix} \tag{14}$$

In other words, the system should attain two conditions simultaneously. First, the position of both sides must be the same. Second, the law of action-reaction. For conventional bilateral teleoperation, the operator at the master side should feel the reflecting force from the environment vividly [12]. For the proposed bilateral control, the system can almost achieve perfect transparency condition when the spring stiffness is high while the damping coefficient is low.

The performance of the teleoperation system is usually evaluated in two motions: *free motion* and *contact motion*. For free motion or non-contact motion, the external torque on slave side is normally considered as zero ($\tau_s = 0$). Thus, the hybrid parameter which is associated with τ_s, H_{12} and H_{22}, should not be effective and transparency should depend on the dynamics of H_{11} and H_{21}. However, the system may have friction components that affect the transparency of the system. For contact motion, all hybrid parameters have influence on the system performance.

IV. VIBRATION SUPPRESSION DESIGN

A. Parameters Selection and Design

In this paper, the system is assumed to be disturbed by external vibration noise from the environment. Accordingly, the disturbance suppression performance of the proposed bilateral control system can be analyzed from the hybrid parameter, H_{22}, which represents the relationship of position response, θ^{res} and external torque input, τ_{ext} as shown in (15).

$$\frac{\theta^{res}}{\tau_{ext}} = \frac{1}{(J + J_v)s^2 + B_v s + K_v} \tag{15}$$

For vibration suppression design, the value of the virtual parameters: J_v, B_v, and K_v, can be determined from the second-order characteristic equation. In this paper, the characteristic equation is established from two poles: g_1 and g_2, that represent the desired cut-off frequencies of the system for disturbance suppression purpose. Hence, the desired second-order characteristic equation of the system is (16).

$$s^2 + (g_1 + g_2)s + (g_1 * g_2) = 0 \tag{16}$$

When compare the characteristic equation of (15) with (16), three virtual parameters must be defined. Thus, one parameter must be assigned beforehand. From the previous section, the value of spring stiffness has an influence on transparency of the system. Therefore, in this paper, the virtual spring stiffness, K_v, is set by the user and the other virtual parameters: damping coefficient, B_v, and inertia, J_v, can be calculated from (17) and (18), respectively.

$$B_v = \left(\frac{g_1 + g_2}{g_1 * g_2} \right) K_v \tag{17}$$

$$J_v = \left(\frac{1}{g_1 * g_2} \right) K_v - J \tag{18}$$

For the concept of spring stiffness selection, the system behaviour with different *interconnected functions* between master and slave system [13], can explain the concept. This function has a direct effect on haptic sense. For the proposed bilateral controller, the variation of spring stiffness influences the type of function; *rigid coupling* or *spring coupling*. With high-stiffness spring, the function is expected to act as rigid coupling which can achieve high transparency as mentioned in the previous section. In contrast, the function should work as spring coupling when the spring stiffness is low.

B. Vibration Suppression Performance Analysis

Assume that the one DOF master and slave manipulator in this paper are identical. Internal friction is small and neglected in this analysis. The desired cut-off frequencies for vibration suppression and the virtual element parameters are selected and calculated. The system parameters are shown in Table I.

TABLE I.   SYSTEM PARAMETERS

Parameters	Symbol	Value	Unit
Master-Slave manipulator			
Master inertia	J_m	0.0001	kg m^2
Slave inertia	J_s	0.0001	kg m^2
Desired cut-off frequencies			
1st cut-off frequency	g_1	50	rad/s
2nd cut-off frequency	g_2	500	rad/s
Virtual parameters			
Spring stiffness	K_v	2.5 – 20	N m/rad
Damping coefficient	B_v	0.055 – 0.44	N m/(rad/s)
Virtual inertia	J_v	0.0 – 0.0007	kg m^2

Fig. 4 depicts the frequency response of (15) with the several virtual parameters sets defined from the variation of virtual spring stiffness, $K_v = 2.5$, 5.0, 10.0, and 20.0 N m/rad. The unit of this equation represents the inverse value of the spring stiffness, in other words, the *compliance* of the system. Especially, this compliance has the dynamics value depends on the frequency of the external torque input.
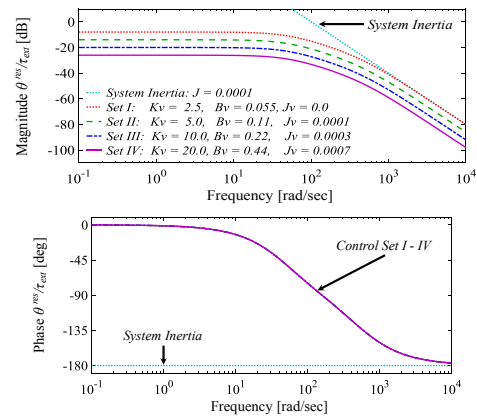

Figure 4.   Bode diagram of disturbance suppression.

(a) 10 Hz   (b) 30 Hz
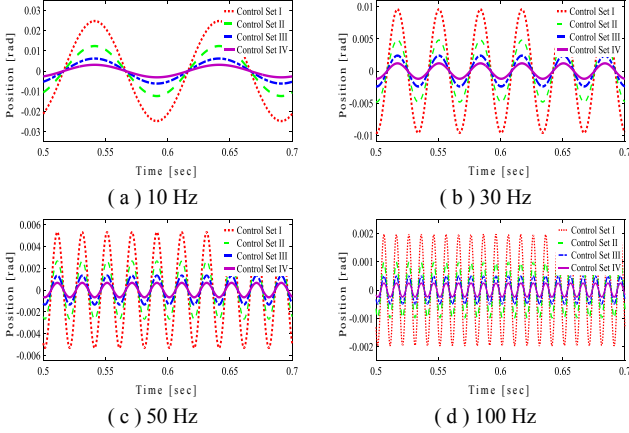
(c) 50 Hz   (d) 100 Hz

Figure 5. Position responses to various frequencies vibration.

In details, the system compliance is controlled by the value of the virtual elements. For Control Set I ($K_v = 2.5$, $B_v = 0.055$, $J_v = 0.0$), the magnitude plot has the constant compliance value at -7.96 dB for low-frequency torque input which corresponds to the spring stiffness, $K_v = 2.5$ N·m/rad. For high-frequency input, the stiffness is stiff after the first cut-off frequency, *50 rad/s or 7.96 Hz*, and similar to the system inertia when the input frequency is higher than the second desired cut-off frequency, *500 rad/s or 79.58 Hz*, without the virtual inertia. As a result, the position response to the high-frequency external torque is reduced due to the lower compliance. For the other control sets, when the spring stiffness is increased, the system compliance in low-frequency range is moved downwards but the desired cut-off frequencies can be maintained because the damping coefficient and inertia are increased as calculated from (17) and (18), respectively. The phase plot in Fig. 4 can confirm the same phase response of all control sets as designed.

The position responses to the various frequencies torque vibration are shown in Fig. 5 (a)-(d). With torque amplitude at 0.1 N·m, the frequency is varied from 10 Hz to 100 Hz. The results demonstrate the performance of the system that can reduce the influence of vibration noise effectively. The higher frequency noise has the lower position response in the system.

V. SIMULATION

A. Simulation Setup

1) Bilateral control system

From the control diagram in Fig. 3, the human and environment is modelled as a spring-damper ($K = 200.0$ N/m and $B = 4.0$ N·s/m). However, the slave manipulator is not in contact with the environment in free motion. Therefore, the environment parameters are not applied but modelled with small a value of damping coefficient, $B_{env} = 0.01$ N·s/m, which resembles the viscous friction.

The master-slave system parameters are identical as defined in Table I and have a length of the link 0.1 m. For more practical results, the external torque is measured by

utilizing the Reaction Torque Observer (RTOB) [14]. In RTOB, the cut-off frequency is set at 5,000 rad/s.

(a) H_{11} (b) H_{12}
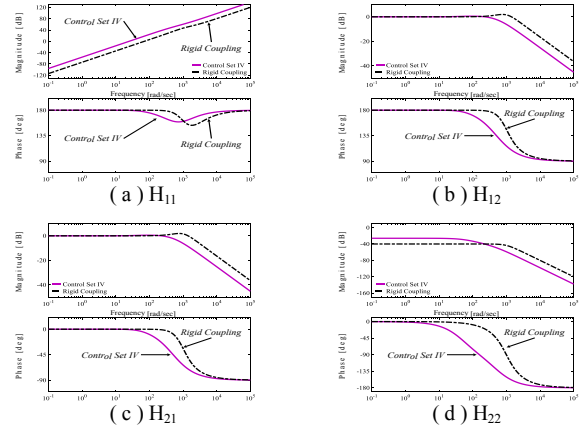
(c) H_{21} (d) H_{22}

Figure 6. Bode diagrams of the hybrid parameters.

For proposed bilateral controller, in this section, the Control Set IV ($K_v = 20.0$, $B_v = 0.44$, $J_v = 0.0007$) is applied for the simulation as the spring coupling control.

2) Rigid coupling control

In section IV, the system transparency can be attained when using high-stiffness value or physical acting as rigid coupling. This paper defines the rigid coupling control with the following parameters: $K_v = 100.0$, $B_v = 0.15$, $J_v = 0.0$.

The comparison of rigid coupling control with the proposed control is demonstrated by Bode diagram of all hybrid parameters in Fig. 6. The bandwidth of rigid coupling control is larger than the proposed control which represents the higher compliance of the system for high-frequency input.

B. Simulation Scenario and Results

The master system is moved by the operator to follow the desired path, which resembles 0.11 Hz sinusoidal wave. The slave system starts touching the object at $t = 4.545$ sec. During the simulation, the slave manipulator is disturbed by mixed-frequencies, 10-100 Hz, torque vibration noise.

1) Position response

The responses in free motion of both controls for low-frequency moving path are the same as shown in Fig. 7 (a) and 8 (a). However, the magnified images in Fig. 7 (c) and 8 (c) demonstrate the difference. The response of proposed control is less sensitive to vibration noise than the rigid coupling control because the effect of virtual damping and inertia that strengthen the robustness of the proposed control for high-frequency disturbance. In contact motion, the response clearly presents the different behavior of two systems. The position gap occurs due to the stiffness of the system. With higher stiffness value, the gap is closer as depicted in Fig. 9.

2) Torque response – Reflection Torque

Fig. 7 (b) and 8 (b) illustrate the slave torque (estimated torque from environment by using RTOB) and reflection torque of two controls. Fig. 7 (d) shows the better result of proposed control that can suppress the effect of high-

frequency noise from environment to the master side while rigid coupling reflects the reaction torque from environment to the human vividly as shown in Fig. 8 (d).
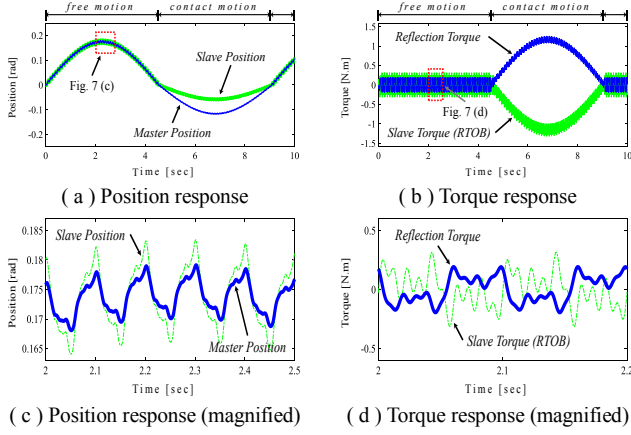

(a) Position response (b) Torque response

(c) Position response (magnified) (d) Torque response (magnified)

Figure 7.   Simulation results of bilateral control
Control Set IV: $K_v = 20.0$, $B_v = 0.44$, $J_v = 0.0007$

(a) Position response (b) Torque response

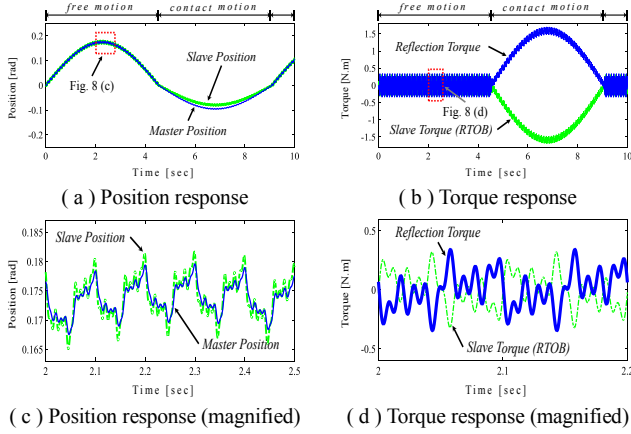(c) Position response (magnified) (d) Torque response (magnified)

Figure 8.   Simulation results of bilateral control
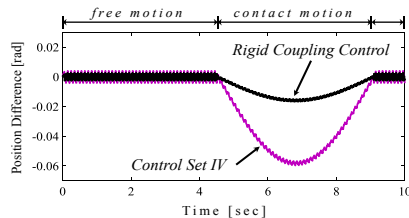Rigid Coupling: $K_v = 100.0$, $B_v = 0.15$, $J_v = 0.0$

Figure 9.   Position Difference: Control Set IV and Rigid Coupling

VI.   CONCLUSION

In this paper, the concept design of vibration suppression in bilateral teleoperation by using the virtual spring-damper system with additional inertia is proposed. For vibration suppression design, the cut-off frequencies and spring stiffness of the system are defined by the user beforehand from the system requirements. The other virtual parameters can be calculated from the equations in order to maintain the desired cut-off frequencies when the stiffness is changed.

The vibration control performance is analyzed from Bode diagram of the hybrid parameter, H_{22}, and position responses to the various high-frequencies torque noise. In simulation, the result of position and reflection torque responses between the proposed bilateral control and rigid coupling control were compared. The master-slave system with both controllers have almost the same movement in free motion. However, the proposed controller demonstrated better performance in noise suppression that reduces vibration from the environment. The low-vibration sensation was reflected to the human. In contact motion, the difference of spring stiffness causes the position gap between master and slave. The proposed bilateral control can be applied for the tasks that require the spring behavior with vibration control such as soft material handling.

REFERENCES

[1]   S. Lichiardopol, "A survey on teleoperation," Dynamic and Control Group, Dept. Mech. Eng., Eindhoven University of Technology, Eindhoven, Netherlands, December 2007.

[2]   Peter F. Hokayem, and Mark W. Spong, "Bilateral teleoperation: An historical survey," *Automatica*, vol. 42, pp. 2035-2057, 2006.

[3]   G. J. Raju, G. C. Verghese and T. B. Sheridan, "Design issues in 2-port network models of bilateral remote manipulation," *Robotics and Automation, 1989. Proceedings., 1989 IEEE International Conference on*, Scottsdale, AZ, vol.3, pp. 1316-1321, 1989.

[4]   B. Hannaford, "A design framework for teleoperators with kinesthetic feedback," in *IEEE Transactions on Robotics and Automation*, vol. 5, no. 4, pp. 426-434, Aug 1989.

[5]   D. A. Lawrence, "Stability and transparency in bilateral teleoperation," in *IEEE Transactions on Robotics and Automation*, vol. 9, no. 5, pp. 624-637, Oct 1993.

[6]   K. Ohnishi, M. Shibata and T.Murakami, "Motion control for advanced mechatronics," in *IEEE/ASME Transactions on Mechatronics*, vol. 1, no. 1, pp. 56-67, March 1996.

[7]   M. Mizuochi, T. Tsuji and K. Ohnishi, "Improvement of disturbance suppression based on disturbance observer," *9th IEEE International Workshop on Advanced Motion Control, 2006.*, Istanbul, 2006, pp. 229-234.

[8]   M. P. Menikdiwela and A. M. H. S. Abeykoon, "Vibration suppression of bilateral control system," *2014 11th International Conference on Electrical Engineering/Electronics, Computer, Telecommunications and Information Technology (ECTI-CON)*, Nakhon Ratchasima, 2014, pp. 1-6.

[9]   L. Chan, F. Naghdy and D. Stirling, "Application of Adaptive Controllers in Teleoperation Systems: A Survey," in *IEEE Transactions on Human-Machine Systems*, vol. 44, no. 3, pp. 337-352, June 2014.

[10]   M. K. Madawala, A. M. H. S. Abeykoon, B. G. C. Mihiran, D. C. Mohottige, R. G. U. I. Meththananda and M. Branesh Pillai, "Virtual torsional spring based bilateral control system for soft manipulation," *2013 International Conference on Circuits, Power and Computing Technologies (ICCPCT)*, Nagercoil, 2013, pp. 337-343.

[11]   H. Li, K. Tadano and K. Kawashima, "Experimental validation of stability and performance for position-error-based tele-surgery," *2015 IEEE International Conference on Advanced Intelligent Mechatronics (AIM)*, Busan, 2015, pp. 848-853.

[12]   A. M. Harsha S. Abeykoon and R. M. M. Ruwanthika. "Remote Gripping for Effective Bilateral Teleoperation," in *Handbook of Research on Human-Computer Interfaces, Developments, and Applications*, Hershey, PA: IGI Global, 2016, ch. 5, pp. 99–134

[13] T. Tsuji, K. Natori, H. Nishi, and K. Ohnishi, "Controller design method of bilateral control system," *Eur. Power Electron. Drives J.*, vol. 16, no. 2, pp. 22–28, 2006.

[14] S. Katsura, Y. Matsumoto and K. Ohnishi, "Modeling of Force Sensing and Validation of Disturbance Observer for Force Control," in *IEEE Transactions on Industrial Electronics*, vol. 54, no. 1, pp. 530-538, Feb. 2007.